Frequent inactivation of *SLIT2* and *ROBO1* signaling in head and neck lesions: clinical and prognostic implications

Guru Prasad Maiti, PhD,[a,b] Amlan Ghosh, PhD,[c] Pinaki Mondal, PhD,[d] Susmita Ghosh, PhD,[a,e] Jayanta Chakraborty, MS,[f] Anup Roy, MD,[g] Susanta Roychowdhury, PhD,[h] and Chinmay Kumar Panda, PhD[a]

Chittaranjan National Cancer Institute, Kolkota, India; University of Kalyani, Nadia, India; Presidency University, Kolkata, India; National Brain Research Centre, Haryana, India; Johns Hopkins School of Medicine, Baltimore, MD, USA; Chittaranjan National Cancer Institute, Kolkata, India; North Bengal Medical College, West Bengal, India; and CSIR-Indian Institute of Chemical Biology, Kolkata, India

Objective. The protein *SLIT2* and its receptor *ROBO1* regulate different cellular processes, such as proliferation, apoptosis, and migration. In this study our aim is to understand the alterations of these genes during development of head and neck squamous cell carcinoma (HNSCC).

Materials and Methods. First, molecular alterations of the genes were analyzed in 30 dysplastic lesions, 128 primary HNSCC samples, and 1 HNSCC cell line. Then alterations were correlated with mRNA expression (n = 22) and protein expression (n = 29). Finally, the alterations were correlated with different clinicopathologic parameters and clinical outcomes of the patients.

Results. *ROBO1* had a comparatively high frequency of deletion (28.5%-54.2%) from dysplastic lesions and subsequent clinical stages than did *SLIT2* (16.6-27%). On the contrary, *SLIT2* had a high frequency (56.6%-81.2%) of promoter methylation from dysplastic lesions onward compared with *ROBO1* (20%-32.8%). Interestingly, alterations of *SLIT2* and *ROBO1* were high in dysplastic lesions (80%), followed by comparable frequencies (92.5%-95.3%) in subsequent stages of tumor. Alterations of these genes showed concordance with their mRNA/protein expression and significant association with poor patient outcome.

Conclusions. Our data suggest that inactivation of *SLIT2* and/or *ROBO1* is one of the early events in development of dysplastic lesions of head and neck and has prognostic importance. (Oral Surg Oral Med Oral Pathol Oral Radiol 2015;119:202-212)

Head and neck squamous cell carcinoma (HNSCC) is the sixth most common cancer worldwide, and it accounts for 30% to 40% of all cancer types in the Indian subcontinent.[1,2] Epidemiologic studies have linked tobacco, betel-nut leaf quid, alcohol, and infection with oncogenic-type human papillomavirus (HPV) 16 and HPV-18 to the development of HNSCC.[1,3] Despite new treatment modalities such as radiotherapy and chemotherapy, HNSCC is associated with high rates of recurrence and mortality, with 5-year survival rates of approximately 50%.[4] Therefore details of the genetic and epigenetic events leading to development of HNSCC should be analyzed to help design novel diagnostic and therapeutic procedures that can be used in the clinical management of the disease.

In a preliminary tumor progression model of HNSCC, allelic loss in the chromosome 3p region was suggested to be associated with the transition of hyperplasia to dysplasia.[5] Our previous study of HNSCC in Indian patients found a high frequency of loss of heterozygosity (LOH) in the chromosome 3p12-13 region and its association with the development of dysplastic lesions.[6] Chromosome 3p12-13 harbors a candidate gene Roundabout1 or Deleted in U

Statement of Clinical Relevance

In the analysis of alterations of *SLIT2* and its receptor *ROBO1* in the development of head and neck squamous cell carcinoma (HNSCC), frequent inactivation of these genes were evident in head and neck lesions. Alterations of these genes were determinant of poor patient outcome.

Disclosures: We are thankful to the Director, Chittaranjan National Cancer Institute, Kolkata, India, for active encouragement and support during this work. Financial support for this work was provided by grants from Department of Biotechnology (BT/PR/5524/Med/14/649/2004), Government of India, to Dr. C. K. Panda and Dr. S. Roychoudhury, Council for Scientific and Industrial Research-Project (IAP-001), Government of India to Dr. S. Roychoudhury, and CSIR-SRF Fellowship (grant no. 09/30 (0053)2 k9-EMR-I) to Mr, Guru Prasad Maiti. The funding sources had no role in writing this manuscript. We also acknowledge Subhayan Sur and Debolina Pal for technical assistance during some of the experiments.

[a]Department of Oncogene Regulation, Chittaranjan National Cancer Institute, Kolkata, India.
[b]Department of Molecular Biology and Biotechnology, University of Kalyani, Nadia, India.
[c]Department of Biological Science, Presidency University, Kolkata, India.
[d]National Brain Research Centre, Manesar, Gurgaon, Haryana, India.
[e]Department of Pathology, Johns Hopkins School of Medicine, Baltimore, Maryland, USA.
[f]Department of Surgical Oncology, Chittaranjan National Cancer Institute, Kolkata, India.
[g]North Bengal Medical College, Sushruta Nagar, Darjeeling, West Bengal, India.
[h]Cancer Biology and Inflammatory Disorder Division, CSIR-Indian Institute of Chemical Biology, Kolkata, India.

Received for publication Jan 17, 2014; returned for revision Sep 10, 2014; accepted for publication Sep 15, 2014.

2212-4403
http://dx.doi.org/10.1016/j.oooo.2014.09.029

Table I. Clinicopathologic features of 158 head and neck lesions

Clinical features	Number of samples (n = 158) (n%)	HPV-16/HPV-18 positivity (%)
Age group		
20-30	3 (1.8)	0 (0)
31-40	29 (18.3)	14 (48.2)
41-50	43 (27.2)	22 (51.1)
51-70	83 (52.5)	49 (59)
Primary sites		
BM	106 (67.08)	58 (54.7)
ALV	22 (13.9)	11 (50)
Sex TNG	30 (18.9)	16 (53.3)
Male	116 (73.4)	63 (54.3)
Female	42 (26.6)	22 (52.3)
Tumor stage		
Mild dysplasia	9 (5.6)	3 (33.3)
Moderate dysplasia	14 (8.8)	7 (50)
Severe dysplasia	7 (4.4)	3 (42.8)
TNM stage I	7 (4.4)	1 (14.2)
TNM stage II	37 (23.4)	22 (59.4)
TNM stage III	44 (27.8)	26 (59)
TNM stage IV	40 (25.3)	23 (57)
Tumor differentiation		
WDSCC	80 (50.6)	42 (52.5)
MDSCC	44 (27.8)	25 (56.8)
PDSCC	4 (2.5)	4 (100)
Lymph node		
Positive	44 (27.8)	24 (54)
Negative	84 (53.1)	47 (55.9)
Etiologic factor		
Tobacco +*	125 (79.1)	65 (52)
Tobacco −	33 (20.8)	20 (60.6)
Alcohol +	16 (10.1)	7 (43.7)
Alcohol −	142 (89.8)	78 (54.9)
HPV-16	80 (50.6)	—
HPV-18	5 (3.1)	—

ALV, alveolus; *BM,* buccal mucosa; *HPV,* human papillomavirus; *TNG,* tongue; *TNM,* tumor node metastasis; *MDSCC,* moderately differentiated squamous cell carcinoma; *PDSCC,* poorly differentiated squamous cell carcinoma; *WDSCC,* well-differentiated squamous cell carcinoma.
* Smoking or chewing tobacco or both.

Twenty-Twenty (*ROBO1/ DUTT1),* a Drosophila homolog gene that encodes a member of the neural cell adhesion molecule (NCAM) in the immunoglobulin (Ig) superfamily.[7] Mice harboring deletions of exon 2 of *ROBO1* spontaneously developed bronchial epithelial hyperplasia, indicating it as a candidate tumor suppressor gene (TSG).[8] Our previous study also found a high frequency of molecular alterations (deletion/ methylation) and concordant reduced expression of *ROBO1* in head and neck lesions, indicating importance of this gene in the development of HNSCC.[7]

ROBO1 serves as a receptor of the *SLIT2-ROBO1* signaling pathway. Drosophila homolog *SLIT2* homology 2 *(SLIT2)* protein contains a unique N-terminal tandem of 4 leucine-rich repeat (LRR) domains. The gene *SLIT2* is located at chromosome 4p15.31 region. The LRR domain of *SLIT2* interacts with the extracellular Ig domain of *ROBO1* and this inhibits downstream signaling network, resulting in cell cycle arrest at the G1-S transition, induction of apoptosis, inhibition of cell migration, and invasion.[9,10] Inactivation of *SLIT2* leads to the development of lung adenocarcinoma and lymphoma in mice, indicating it as a candidate TSG.[11] Reduced expression of *SLIT2* has also been reported in carcinomas of the colon, cervix, and lung.[12-15] Therefore *SLIT2* and *ROBO1* are 2 important candidate TSGs of the *SLIT2-ROBO1* signaling pathway and inactivation of either of these candidate genes might lead to inactivation of the said signaling pathway, resulting in development of malignant tumors. To the best of our knowledge, alterations of *SLIT2* have not yet been studied in HNSCC, although frequent deletion of the chromosomal region (4p15.31) harboring the candidate gene has been reported in an HNSCC cell line.[16]

Thus to explore the role of the *SLIT2-ROBO1* signaling pathway in the development of HNSCC, attempts have been made to analyze the alterations (deletion, methylation, mutation, and expression) of *SLIT2* and *ROBO1* in same set of dysplastic and HNSCC samples of Indian patients and in an HNSCC cell line.

The molecular alterations were then correlated with various clinicopathologic parameters and with disease outcomes. Our data revealed that frequent alterations of *SLIT2* in addition to *ROBO1* of the *SLIT2-ROBO1* signaling pathway were associated with the development of HNSCC. The alterations of *SLIT2* and *ROBO1,* along with less advanced clinical stage, were determinants of poor prognosis of the disease.

MATERIALS AND METHODS

Patient population, tumor tissues, and cell line

The Institutional Ethical Board of Chittaranjan National Cancer Institute, Kolkata, India, approved the usage of human specimens in this study. The tumor specimens were collected from the hospital section of Chittaranjan National Cancer Institute, Kolkata, after obtaining written, informed consent from the concerned patients, in stipulated format, approved by the Institutional Ethical Board of Chittaranjan National Cancer Institute, Kolkata, India. The patients are from eastern India. A total of 158 primary tumor tissue samples from oral cavities without any previous treatment as well as matched adjacent normal tissues were collected (Table I). After surgery, all the patients received conventional chemotherapy or radiotherapy or both. Only primary tumor samples from oral cavity were collected. All these tumors were graded and staged according to the Union for International Cancer Control (UICC) tumor node metastasis (TNM) classification. Patient's clinicopathologic information (n = 158) is presented in Table I and Supplemental Table SI (available on the journal's website at www.oooojournal.net). Samples

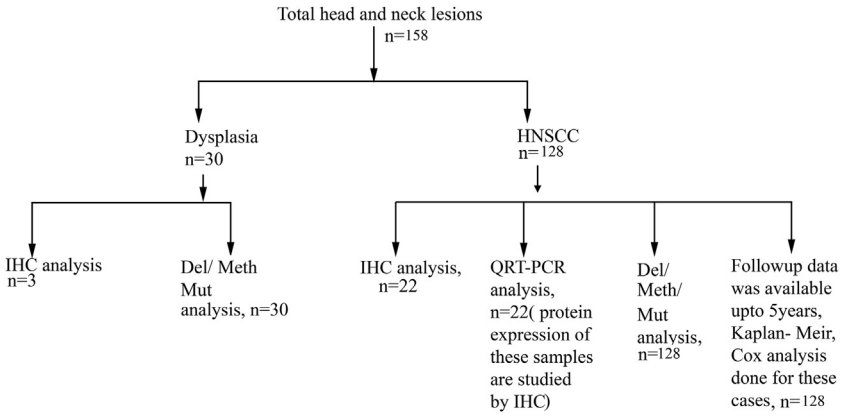

Fig. 1. Tumor samples usage. Schematic representation of the usage of primary head and neck squamous cell carcinoma (HNSCC) tumor in different analyses. *Del,* deletion analysis; *HNSCC,* head and neck squamous cell carcinoma; *IHC,* immunohistochemical analysis; *Meth,* methylation analysis; *Mut,* mutation analysis by SSCP; *n,* sample number; *QRT-PCR,* real-time PCR quantification.

were frozen at −80°C immediately after collection until use. Portions of the freshly operated tissues of some samples (n = 22) were directly collected in TRIzol reagent (Invitrogen, Carlsbad, CA, USA) for RNA isolation, and also parts of some samples (n = 29) were fixed in formalin and embedded in paraffin for immunohistochemical analysis. The cell line UPCI:SCC084, isolated from 52-year-old male Caucasian oral cancer patient with pathologic stage T2 N2 B and with smoking and alcohol habit,[17] was kindly provided by Prof. Susanne M. Gollin (University of Pittsburgh, PA, USA). Summary of the total samples used in different experiments is shown in Figure 1.

Microdissection and DNA extraction

The contaminant normal cells in the head and neck lesions were removed by microdissection procedure from cryosections (5 μm) using surgical knives under a dissecting microscope (Leica MZ16, Wetzlar, Germany). The representative sections from different regions of the specimens were stained with hematoxylin and eosin for diagnosis as well as for marking of the dysplastic epithelium/tumor-rich regions. The samples containing >60% dysplastic epithelium/tumor cells were taken for isolation of DNA according to the standard procedure.[18] High-molecular-weight DNA was extracted by proteinase-K digestion, followed by phenol-chloroform extraction.[19,20]

Deletion analysis

Deletion analysis of *SLIT2* and *ROBO1* loci was done in 30 dysplastic head and neck lesions and 128 HNSCC samples, using microsatellite markers (Supplemental Table SII; available on the journal's website at www.oooojournal.net). Among the samples, deletion of *ROBO1* has been reported in the 25 dysplastic lesions and 72 HNSCC samples in our previous study.[7] In microsatellite-based deletion mapping, polymerase chain reaction (PCR) containing [γ-P32] ATP end labeled forward primer was done in a 20 μL reaction volume according to the method described by Tripathi et al.[21] The microsatellite markers were selected on the basis of their map positions and heterozygosity (Ensembl Release 49, http://www.ensembl.org, 2008). For deletion analysis of *ROBO1*, an intragenic microsatellite marker D3S1274 located in intron-2 and another microsatellite marker D3S3507 located at 89 Kb downstream were used. For deletion analysis of *SLIT2*, an intragenic microsatellite marker D4S1372 and another marker D4S1546 located at 145 kb downstream from *SLIT2* were used. Because D4S1372 was homozygous, multiplex PCR was performed with a control marker D4S2364 having infrequent alterations, as reported by Singh et al.[22] Scoring of loss of heterozygosity [LOH]/deletion and microsatellite size alteration [MA] for informative and noninformative markers were done according to the method described by Tripathi et al.[21]

Promoter methylation analysis

The promoter methylation of *SLIT2* and *ROBO1* genes was analyzed in 30 dysplastic head and neck lesions and 128 HNSCC and corresponding adjacent normal samples by PCR-based methylation-sensitive restriction analysis (MSRA) using MspI/HpaII restriction enzymes (Sibenzyme, Novosibirsk, Russia) as described previously.[23,24] The data obtained by MSRA was validated by methylation-specific PCR (MSP) in 25 randomly selected samples after bisulphite modification of the genomic DNA according to the standard procedure.[25] Details of primer sequences are listed in Supplemental Table SII.

Mutation analysis

The mutation of *SLIT2* and *ROBO1* was screened in 30 dysplastic head and neck lesions, 128 HNSCC samples, and on 1 oral cancer cell line by single-strand

conformation polymorphism (SSCP) analysis using radio labeled [α-P32] deoxycytidine 5′-triphosphate (dCTP) as described by Tripathi el al.[26] The *SLIT2-ROBO1* interacting domains encompassing exons 9 to 14 of *SLIT2* and exons 2 to 4 of *ROBO1* were selected for mutation analysis. All the primers used in this experiment are listed in Supplemental Table SII. Electrophoresis was done in 6% nondenaturing polyacrylamide gel with 10% glycerol at 2 W overnight and autoradiographed on X-ray film (Kodak, Rochester, NY, USA). Sequencing of both strands of samples showing abnormal band shift was done using 3130xl Genetic Analyzer (Applied Biosystems, Foster City, CA, USA).

mRNA expression analysis

mRNA expression of *SLIT2* and *ROBO1* was analyzed in only 22 primary HNSCC samples (because of availability of limited amount of primary tissues after surgery), corresponding adjacent normal tissues, and HNSCC cell line SCC084 using primers, as mentioned in Supplemental Table SII. Total RNA was isolated from samples using TRIzol reagent according to the manufacturer's protocol (Invitrogen, Carlsbad, CA, USA). Reverse transcription reaction was performed with 1 μg of total RNA using Random Hexamers (Invitrogen) and M-MuLV Reverse Transcriptase (Promega, Madison, WI, USA). Relative expression of the gene was measured by real-time quantitation using β2-microglobulin (B2M) as an internal control.[24]

Cell line and 5-Aza-deoxycytidine (5-aza-dc) treatment

As in our previous study, the 5-aza-dc concentration was taken up to 20 μM.[23] Subconfluent cultures of SCC084 were treated with 10 μM and 20 μM 5-aza-dc (Sigma-Aldrich, St. Louis, MO, USA) for 5 days. Controls without 5-aza-dc were cultured concomitantly in the same manner. After completion of treatment, cells were harvested, followed by RNA isolation, cDNA preparation, and real-time quantitation using the Power SYBR Green PCR assay kit according to manufacturer's protocol (Applied Biosystems, Foster City, CA, USA).

Immunohistochemical / immunocytochemical analysis

Protein expression of *SLIT2* and *ROBO1* was assessed by immunohistochemical (IHC) analysis in only 25 head and neck lesions and adjacent normal samples (because of limited availability of primary tissue after surgery) and by immunocytochemical (ICC) analysis in the SCC084 cell line according to standard protocol.[23] The tissue sections were incubated overnight at 4° C with primary antibodies *SLIT2* (sc-16619) and *ROBO1* (sc-16611) (Santa Cruz Biotechnology, Santa Cruz, CA, USA) used at a dilution of 1:80. HRP-conjugated rabbit anti-goat secondary antibody (sc-2768) was added at 1:500 dilutions. The slides were developed using 3-3′ diaminobenzidine (DAB, Santa Cruz Biotechnology) as the chromogen, counterstained with hematoxylin, and photographed with a bright-field microscope (Leica DM1000, Wetzlar, Germany). The staining intensity (1 = weak, 2 = moderate, 3 = strong) and the percentage of positive cells (<1 = 0, 1-20 = 1, 20-50 = 2, 50-80 = 3, >80 = 4) were detected by 2 independent observers, and by combining the 2 scores, final evaluation of expression was done (0-2 = low, 3-4 = intermediate, 5-7 = high).[27]

For ICC analysis, cover slip culture of the SCC084 cell line was reacted with the same dilution of primary antibodies of these proteins after permeabilization with 0.5% Triton X-100 and blocking with 5% bovine serum albumin (BSA). After washing, the coverslips were incubated with corresponding FITC-conjugated rabbit anti-goat secondary antibody (sc-2777) at 1:500 dilutions and mounted with glycerol after thorough washing. Imaging of the cover slip was performed with a semiconfocal laser dissecting microscope using Apotome with Axiovision 4.8.1 Software (LCM, Carl Zeiss, Göttingen, Germany). All the chemicals were purchased from Santa Cruz Biotechnology.

Detection of HPV-16 and HPV-18

HPV infection in the head and neck lesions was detected by PCR using primers (MY09 and MY11) from the consensus L1 region followed by typing of HPV-16 and HPV-18 in the L1 positive samples as described by Ghosh et al.[2]

Statistical analysis

Fisher's exact test was used to determine the association between tumors' genetic profile and different clinicopathologic features. All statistical tests were 2-sided and considered significant at $P < .05$. Survival curves were calculated according to the Kaplan-Meier method in 128 HNSCC samples. After sample collection, follow-up data on the patients were taken for up to 5 years and overall survival of the patients was assessed with genetic alterations. According to the hospital-based cancer registry, all the deaths were as a result of cancer-related complications. For this method, *P* values were evaluated by the log rank test for censored survival data. A Cox proportional hazards regression model was used to test the statistical significance of several potential prognostic factors, such as clinical stage, tumor site,

tobacco exposure, HPV infection, and alterations of the candidate TSGs, that were jointly predictive of overall survival of the patients. From this model we estimated the hazard ratio (HR) for each potential prognostic factor with a 95% confidence interval (CI) in multivariate fashion. All the statistical analysis was performed using statistical programs Epi Info 6.04d and SPSS 10.0 (SPSS Inc., Chicago, IL, USA).

RESULTS

Analysis of HPV infection

Infection by HPV is considered one of the important etiologic factors for HNSCC development. HPV typing was done in this study to analyze the frequency of high-risk HPVs in our samples. HPV DNA was detected in 53.7% (85/158) of the tumors (Table I). Among the HPV-positive samples, 94.1% (80/85) were HPV-16 positive and 5.8% (5/85) were HPV-18 positive.

Deletion analysis of *SLIT2* and *ROBO1* loci

In dysplastic lesions, a comparatively higher frequency of deletion was seen in *ROBO1* (28.5%, 8/28) locus than in *SLIT2* (16.6%, 5/30) (Supplemental Table SI). In HNSCC samples, the deletion frequency of *ROBO1* was comparable up to stages I and II (28.50%, 10/35), followed by significant increase ($P = .003$) in stages III and IV (48.6%-54.2%) (Figure 2A, B, C, F). On the other hand, the deletion frequency of *SLIT2* (18%-27%) did not change significantly during progression of tumor. Low frequency of microsatellite size alterations (MAs) was found in both *SLIT2* and *ROBO1* (6.6% to 10%) loci during progression of the tumor (Supplemental Table SI). Deletions of *SLIT2* and *ROBO1* had no significant association (Supplemental Table SIII; available on the journal's website at www.oooojournal.net).

Promoter methylation analysis of *SLIT2* and *ROBO1*

In methylation analysis, concordance was found between MSRA and MSP analyses (Supplemental Table SIV; available on the journal's website at www.oooojournal.net). No promoter methylation was detected in the adjacent normal tissues of the samples. However, in the dysplastic lesions, higher frequency of methylation was found in *SLIT2* (56.6%, 17/30) than in *ROBO1* (20%, 6/30) (Supplemental Table SI). During progression of HNSCC, the methylation frequency of *SLIT2* increased in subsequent stages (75%-81.2%), whereas in *ROBO1* the methylation frequency did not change significantly (27.2%-32.5%) (Figure 2E, F, G). Promoter methylation of both *SLIT2* and ROBO1 was found in SCC084 (Supplemental Table S1). No significant association was found between the methylation status of *SLIT2* and *ROBO1* in dysplastic lesions, but significant association was found in HNSCC samples ($P = .003$) (Supplemental Table SV; available on the journal's website at www.oooojournal.net). This indicates that methylation of *SLIT2* might have some cooperativity in *ROBO1* methylation in HNSCC.

Mutation analysis of *SLIT2* and *ROBO1* interacting domain

Mutation in *SLIT2-ROBO1* interacting domain might disrupt the association of proteins, resulting in deregulation of the signaling network. Thus mutation analysis in *SLIT2* and *ROBO1* interacting domains were analyzed by SSCP analysis (Supplemental Figure S1; available on the journal's website at www.oooojournal.net). No altered band was observed in both *SLIT2* and *ROBO1* interacting regions. Thus mutation in *SLIT2-ROBO1* interacting domains seemed to be a rare event in HNSCC.

Overall alterations of *SLIT2* and *ROBO1*

The overall alterations (deletion/methylation) of the genes in the tumors were: Dysplasia: *SLIT2* (63.3%; 19/30), *ROBO1* (43.3%; 13/30); HNSCC: *SLIT2* (84.3%; 108/128), *ROBO1* (57.8%; 74/128). In HNSCC samples, overall alteration frequency of *SLIT2* was almost constant in subsequent stages of the disease. The overall alteration frequency of *ROBO1* was comparable up to stages I and II (43.1%, 19/44), followed by significant increase ($P = .01$) in stages III and IV (63.6%-67.5%) (Figure 2H, Supplemental Table SVI; available on the journal's website at www.oooojournal.net). However, alteration of the gene was not associated with nodal status, HPV infection, or tobacco habit. The majority of the tumors (80.3%; 127/158) had epigenetic/genetic alterations in at least 1 of the genes, with high frequency of alterations in dysplastic lesions (80%, 24/30), followed by comparable frequencies (92.5%-95.3%) during progression of the tumor (Figure 2G, Supplemental Table SI). This suggests that deregulation of the *SLIT2-ROBO1* signaling is one of the early events in the development of this tumor.

mRNA expression of *SLIT2* and *ROBO1* in HNSCC

In quantitative RT-PCR analysis, *SLIT2* and *ROBO1* had greater than 2-fold reductions in mRNA expression in 91% (20/22) and 54% (12/22) of tumors, respectively (Figure 3A, B). The frequency of the samples with mean fold reduction in mRNA expression of *SLIT2* was greater than that of *ROBO1*. Both *SLIT2* and *ROBO1* mRNA expression was downregulated in the SCC084 cell line. Thus, mRNA expression of *SLIT2* and *ROBO1* was severely impaired in HNSCC.

To confirm inactivation of the *SLIT2* and *ROBO1* because of methylation, a demethylation experiment was performed by treatment of 5-aza-dc in the SCC084 cell line. Upregulation of *SLIT2* and *ROBO1* mRNA

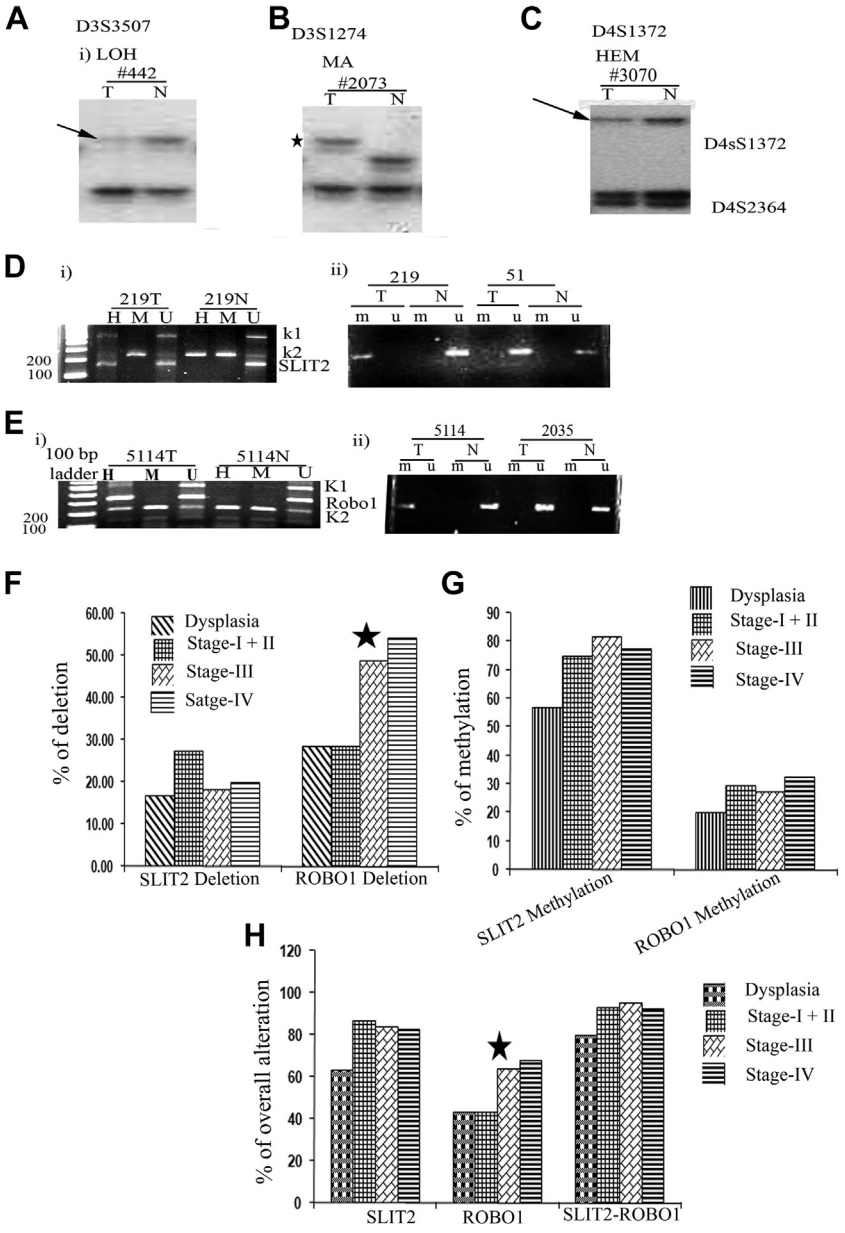

Fig. 2. Molecular alterations of *SLIT2* and *ROBO1*. Representative autoradiographs showed the deletion and microsatellite size alteration (MA) of *ROBO1* and *SLIT2* locus. (**A**) Loss of heterozygosity (LOH) at D3S3507 in sample 442; (**B**) MA-I of the microsatellite at D3S1274 in sample 2073; (**C**) hemizygous deletion (HEM) at D4S1372 in sample 3070. The marker D4S2364 was used as internal control for multiplex PCR. (**D**) Representative gel electrophorogram showing the methylation status of *SLIT2* in tumor samples and in corresponding normal sample (i) by methylation-sensitive restriction analysis (MSRA) and (ii) validated by methylation-specific PCR (MSP) after bisulphate modification of DNA. (**E**) Representative gel electrophorogram showing the methylation status of *ROBO1* in tumor samples and in corresponding normal sample (i) by MSRA and (ii) validated by MSP. The samples 219 T and 5114 T had the methylation-specific PCR band, but 219 N, 5114 N, 51 TN, and 2035 TN had an unmethylation-specific PCR band. *K1* and *K2*: controls for DNA digestion and integrity, respectively; *H,* amplicon obtained with primer for HpaII digested DNA; *M,* amplicon obtained with primer for MspI digested DNA; *U,* amplicon obtained with primer for undigested DNA. u; amplicon obtained with primer for modified unmethylated DNA; *m,* amplicon obtained with primer for modified methylated DNA; *T,* tumor DNA; *N,* corresponding normal tissue DNA. (**F**) Bar diagram indicates the stage-wise deletion pattern of *SLIT2* and *ROBO1* locus. Star marks indicate the significant difference. (**G**) Bar diagram shows the stage-wise methylation pattern of *SLIT2* and *ROBO1*. (**H**) Bar diagram represents the stage-wise overall alteration pattern of individual genes and *SLIT2-ROBO1* receptor ligand.

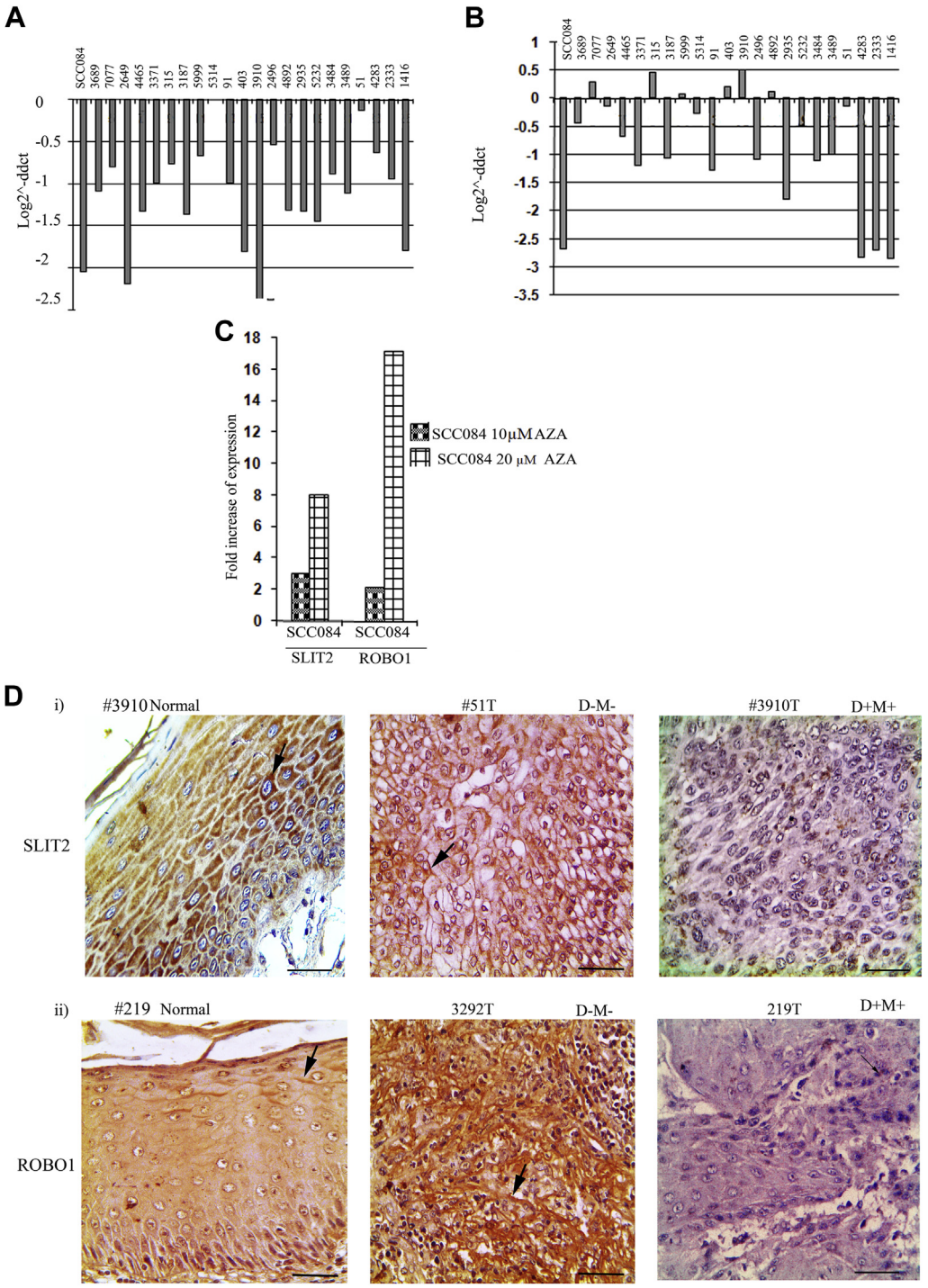

Fig. 3. Expression analysis of *SLIT2* and *ROBO1*. Quantitative RT-PCR indicating mRNA expression pattern of (**A**) *SLIT2* (**B**) *ROBO1* in HNSCC samples and cell line. Bars represent the gene expression normalized to β2-microglobulin and relative to corresponding adjacent normal tissues, using 2^{-ddCt} method. X-axis indicates the sample numbers. (**C**) Bar diagram indicates the effect of 5-aza-dc treatment on *SLIT2* and *ROBO1* expression in SCC084 cell line. The expression level of both *SLIT2* and *ROBO1* was increased in the cell line. (**D**) (i) Differential cytoplasmic expression of *SLIT2* in the basal lining/parabasal cells of normal oral epithelium and primary HNSCC samples were found. Spinous layer had high expression of *SLIT2*. Tumor sample 51 T had high expression and 3910 T had low expression of *SLIT2*. (ii) Distinct membrane expression of *ROBO1* was found in parabasal/spinous layer cells and cytoplasmic expression in basal lining of normal oral epithelium. Tumor sample 3292 had high cytoplasmic and membrane expression of *ROBO1*. Sample 219 T had low expression of the gene and tumor samples. Magnification of tissue samples is 40×. Scale bar represent 50 μm. Black arrowhead indicates the localization of the protein. *D+/−*, deletion present/absent; *M+/−*, methylation present/absent.

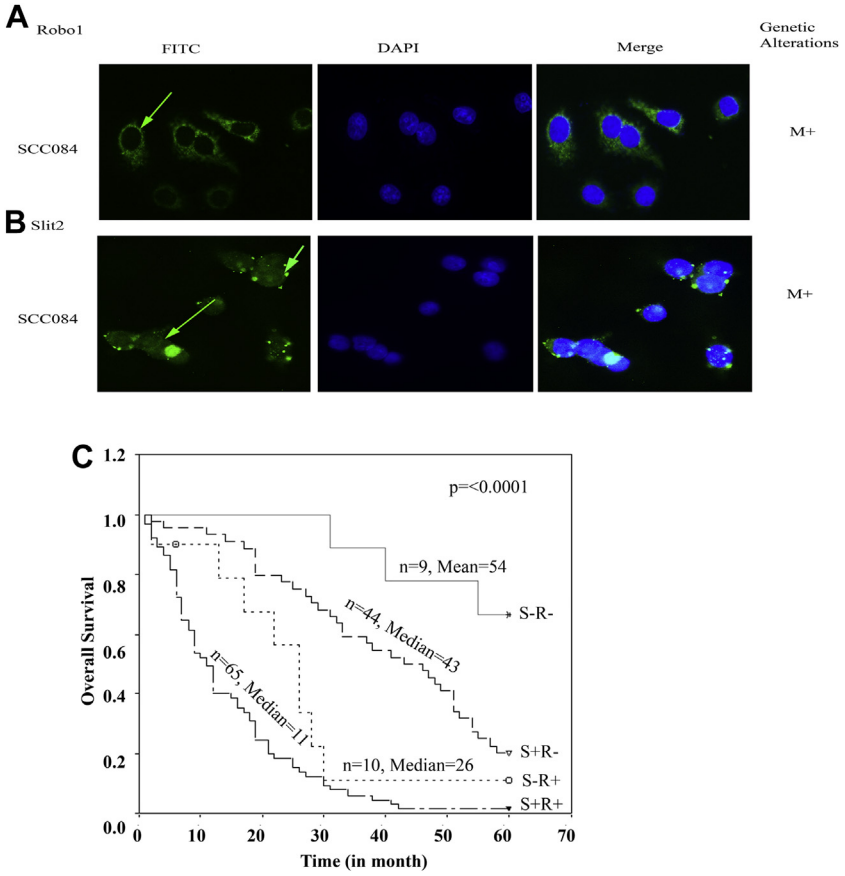

Fig. 4. Immunocytochemical (ICC) analysis of *SLIT2* and *ROBO1*. Overnight subconfluent cover slip culture of SCC084 cell line was fixed with 100% methanol and protein expression of the genes was analyzed by ICC. (**A**) *ROBO1* had reduced cytoplasmic expression in SCC084. (**B**) *SLIT2* expression was low with membrane aggregation in SCC084. Green arrows indicate the protein expression and localization. *M+/−,* methylation present/absent. (**C**) Kaplan-Meier analysis of survival (up to 5 years) of HNSCC patients. Alteration of both *SLIT2* and *ROBO1* was significantly associated with poor overall survival (OS) with log rank $P = .0001$. Survival time was defined as the time from the date of surgery to the date of last follow-up (up to 5 years). *n,* number of samples; *S+R+,* patients with genetic/epigenetic alteration of both *SLIT2* and *ROBO1*; *S+R−,* patients with genetic/epigenetic alteration of *SLIT2* without *ROBO1* alteration; *S−R+,* patients with genetic/epigenetic alteration of *ROBO1* without *SLIT2* alteration; *S−R−,* patients having no alteration of *SLIT2* and *ROBO1*.

expression as a result of 5-aza-dc treatment was observed in the cell line with respect to untreated controls. In presence of 5-aza-dc (20 µm), About 9 fold activation of *SLIT2* and 18 fold activation of *ROBO1* were observed in SCC084 (Figure 3C). Thus promoter methylation might be one of the inactivating mechanisms of reduced expression of the genes.

Analysis of *SLIT2* and *ROBO1* protein expression

In normal oral epithelium, diffuse low cytoplasmic expression of *SLIT2* in the basal layer and high cytoplasmic expression in the spinous layer were noted (Figure 3D), whereas *ROBO1* had diffuse cytoplasmic expression in the basal/parabasal layer and distinct membrane expression in spinous layer (Figure 3D). In primary tumors, moderate/low expression of *SLIT2* and *ROBO1* was found in 89% (26/29) and 58% (17/29) of samples, respectively (Figure 4A). Reduced cytoplasmic expression of *ROBO1* was observed in SCC084. Reduced cytosolic expression of *SLIT2* was seen in SCC084 with discrete membrane foci (Figure 4B). This might be due to some modifications of these receptors and ligands in the cell line leading to their aggregation on the nucleus and membrane.

In correlation analysis, significant association was found between reduced expression (mRNA/proteins) of the genes and their molecular alterations (Table II).

Clinicopathologic association of *SLIT2* and *ROBO1*

The alterations of *SLIT2* and *ROBO1* were correlated with the clinicopathologic/survival parameters in order to uncover their prognostic significance (if any) for early diagnosis and prediction of patient outcome. The Kaplan-Meier (K-M) analysis revealed significantly

Table II. Correlation of molecular alterations with RNA/protein expression of the genes *SLIT2* and *ROBO1*

	SLIT2					*ROBO1*		
	expression					*expression*		
	RNA	*Protein*	*Genetic alteration*	*Node*	*HPV*	*RNA*	*Protein*	*Genetic alteration*
HNSCC cell line								
SCC084	↓↓	+	M+	ND	16/18	↓↓	+	M+
Dysplasia								
L61	ND	+++	D−M−	ND	16	ND	+	D+M+
L53	ND	+	D−M+	ND	A	ND	++	D−M+
L60	ND	++	D−M+	ND	16	ND	+	D+M−
Tumor samples								
3689	↓↓	++	D−M+	+	A	↓	+	D−M+
7077	↓	++	D−M+	−	16	Normal	+++	D−M−
2649	↓↓	++	D−M+	−	16	Normal	++	D−M−
4465	↓↓	++	D−M+	+	A	↓	++	D−M+
3371	↓	++	D−M+	−	A	↓↓	+	D−M+
315	↓	++	D−M+	+	A	Normal	+++	D−M−
3187	↓↓	+	D+M+	−	16	↓↓	++	D−M+
5999	↓	+	D−M+	−	16	Normal	+++	D−M−
6835	↓	++	D−M+	−	A	↓↓	+	D+M+
403	↓↓	++	D−M+	−	16	Normal	+++	D−M−
3910	↓↓	+	D+M+	−	16	Normal	+++	D−M−
2496	↓↓	++	D−M+	−	A	↓	++	D−M+
4892	↓↓	++	D−M+	−	A	Normal	+++	D−M−
2935	↓↓	++	D−M+	+	16	↓↓	++	D−M+
5232	↓↓	++	D−M+	+	A	↓	+	D−M+
3484	↓	+	D−M+	+	16	↓↓	++	D−M+
3489	↓↓	++	D−M+	−	18	↓↓	+	D−M+
51	Normal	++	D−M−	+	A	Normal	+++	D−M−
4283	↓	++	D−M+	+	A	↓↓	+	D+M+
2333	↓	++	D−M+	+	A	↓↓	+	D+M−
1416	↓↓	+	D−M+	+	16	↓↓	+	D+M+
4546	↓	++	D−M+	−	A	Normal	+++	D−M−
P value	.0085						> .001	

A, HPV absent; *D+/−,* deletion (microsatellite size alteration [MA], loss of heterozygosity [LOH]) positive/negative; *M+/−,* methylation positive/negative; *ND,* not determined; *HNSCC,* head and neck squamous cell carcinoma; *16/18,* HPV-16/HPV-18; ↓, decreased gene expression compared with normal; +++, protein expression high; ++, protein expression medium, +, protein expression low.
Statistically significant ($P < .05$).

reduced overall survival (OS) of HNSCC patients with alterations of both *SLIT2* and *ROBO1* (log rank $P = .0001$) (Figure 4C). Interestingly, alterations of either *SLIT2* or *ROBO1* also predicted poorer OS of the patients than the patients having no alterations (Figure 4C). The Cox regression analysis indicated that alterations of *SLIT2* (HR: 2.8117, CI: 1.4792-5.3444) and *ROBO1* (HR: 6.4368, CI: 3.8981-10.6290) with lower clinical stage (HR: 0.7912, CI: 0.6346-0.9864) of the disease were determinant of poor prognosis of HNSCC patients (Table III), thereby enabling efficient classification of the high-risk patients. Other clinicopathologic parameters, such as HPV, tobacco, alcohol, and lymph node metastasis, have no significant role in prediction of clinical outcome over histologic grade and alterations of both genes.

DISCUSSION

The aim of this study was to investigate the association of ligand-receptor encoding genes *SLIT2* and *ROBO1* with the development of HNSCC. Infrequent deletion and high frequency of methylation of *SLIT2* in dysplastic head and neck lesions followed by a similar trend in invasive tumors (Figure 2) indicated the importance of epigenetic alteration of the gene in development of the disease. The 5-aza-dc experiment in the UPCI:SCC084 cell line confirmed the inactivation of *SLIT2* by promoter methylation (Figure 3C). To our knowledge, no such study has yet been reported in HNSCC. Frequent methylation of *SLIT2* has also been reported in premalignant and malignant lesions of the cervix, lung, and colon[13,28-30] and also in glioma, ovarian carcinoma, and breast carcinoma.[12-15] In contrast to our data, high frequency of deletion of *SLIT2* has been reported in mesothelioma and carcinomas of lung, breast, and cervix.[13] The differences in the genetic and epigenetic changes of *SLIT2* in HNSCC than other cancers might be due to the differences in molecular pathogenesis of the disease.

Table III. Multivariate analysis of *SLIT2* and *ROBO1* alterations in 128 HNSCC samples with different clinicopathologic parameters

	Overall survival		
Variables	P *value*	*HR*	*95% CI for HR*
Histology	.5365	1.1176	0.7855 - 1.5902
Stage	.0374*	0.7912	0.6346 - 0.9864
HPV	.1967	1.3003	0.8728 - 1.9371
Tobbaco	.7944	0.9373	0.5761 - 1.5251
Alcohol	.5267	1.2454	0.6312 - 2.4573
Node	.6104	1.1335	0.6999 - 1.8359
SLIT2 ALT	.0016*	2.8117	1.4792 - 5.3444
ROBO1 ALT	< .00001*	6.4368	3.8981 - 10.6290

HPV, human papillomavirus; *HR,* hazard ratio.
* indicate statistically significant values.

Unlike *SLIT2, ROBO1* had more frequent deletion than methylation in dysplastic and early invasive lesions, with significant increase in later stages of tumor progression (Figure 2F). This suggests association of *ROBO1* inactivation with the development and progression of the disease. Similarly, deletion seemed to be predominant mechanism of inactivation of *ROBO1* over methylation in multiple malignancies such as glioma and carcinomas of the lung, breast, and cervix.[15,28,31] Absence of mutation in the LRR domain (*ROBO1* interacting region) of *SLIT2* and in Ig domain of *ROBO1* (*SLIT2* interacting region) suggests mutation in *SLIT2-ROBO1* interacting domain is a rare event of these genes in HNSCC. High frequency of overall alteration of *SLIT2* or *ROBO1* in dysplastic lesions, and comparable frequency in subsequent stages of the disease, indicate that alterations of *SLIT2-ROBO1* signaling were relatively early to the cancer onset and maintain the same levels of alterations during the tumor progression.

Reduced expression (mRNA) of *SLIT2* and *ROBO1* in the majority of the primary tumors and HNSCC cell line having deletion and/or methylation indicated the importance of these mechanisms in gene inactivation (Figure 3A, B, Table II). The concordance of expression status of the proteins (by IHC) with that of mRNA also supported this phenomenon. Similar findings have also been reported in carcinomas of the cervix, lung, and breast[13,15,28,29]

In our previous study of *ROBO1* alteration (deletion/methylation) in HNSCC development, frequent alteration of *ROBO1* was seen in dysplastic and invasive lesions.[7] In this study, to understand the association of *SLIT2-ROBO1* in the development of HNSCC some common samples of dysplastic lesions (n = 25) and invasive lesions (n = 72) of the previous study were used along with some freshly collected samples (dysplastic lesions: 5; invasive lesions: 56). The *ROBO1* alteration had concordance with the previous study. The alterations of *SLIT2* and *ROBO1* were high (80%) and did not change significantly in later stages of tumor development, indicating the importance of this pathway in the development of HNSCC (Figure 2H). The association of *SLIT2* and *ROBO1* inactivation with poor patient outcome (Figure 4C) suggests their prognostic importance. This has been supported by multivariate analysis where poor prognosis of the patients was found to have alterations of both *SLIT2* and *ROBO1* in the tumors at early clinical stages (Table III).

It was evident that inactivation of *SLIT2-ROBO1* pathway led to the accumulation of activated CDC42-GTP complex, resulting in (i) inactivation of EGFR degradation through endocytosis, (ii) promotion of cell migration by losing the interaction between E-cadherin and β-catenin, (iii) increase of actin polymerization, and so on (Supplemental Figure S2; available on the journal's website at www.oooojournal.net).[9,32,33] This might cause deregulation of different cellular processes such as proliferation, apoptosis, and cell motility,[9] leading to selection of highly malignant clones with adverse prognosis.

CONCLUSIONS

Our study found that frequent alterations of *SLIT2,* in addition to *ROBO1,* of the *SLIT2-ROBO1* signaling pathway was associated with the development of HNSCC. Detailed analysis of this pathway is warranted to find key molecular targets for development of effective therapeutic strategies for management of the disease.

REFERENCES

1. Ferlay J, Shin HR, Bray F, Forman D, Mathers C, Parkin DM. Estimates of worldwide burden of cancer in 2008: GLOBOCAN 2008. *Int J Cancer*. 2010;127:2893-2917.
2. Ghosh A, Ghosh S, Maiti GP, et al. SH3 GL2 and CDKN2 A/2 B loci are independently altered in early dysplastic lesions of head and neck: Correlation with HPV infection and tobacco habit. *J Pathol*. 2009;217:408-419.
3. Leemans CR, Braakhuis BJ, Brakenhoff RH. The molecular biology of head and neck cancer. *Nat Rev Cancer*. 2011;11:9-22.
4. Mondal P, Datta S, Maiti GP, et al. Comprehensive SNP scan of DNA repair and DNA damage response genes reveal multiple susceptibility loci conferring risk to tobacco associated leukoplakia and oral cancer. *PLoS One*. 2013;8:e56952.
5. Perez-Ordonez B, Beauchemin M, Jordan RC. Molecular biology of squamous cell carcinoma of the head and neck. *J Clin Pathol*. 2006;59:445-453.
6. Chakraborty SB, Dasgupta S, Roy A, et al. Differential deletions in 3 p are associated with the development of head and neck squamous cell carcinoma in Indian patients. *Cancer Genet Cytogenet*. 2003;146:130-138.
7. Ghosh S, Ghosh A, Maiti GP, et al. Alterations of ROBO1/DUTT1 and ROBO2 loci in early dysplastic lesions of head and neck: Clinical and prognostic implications. *Hum Genet*. 2009;125:189-198.
8. Xian J, Clark KJ, Fordham R, Pannell R, Rabbitts TH, Rabbitts PH. Inadequate lung development and bronchial

hyperplasia in mice with a targeted deletion in the Dutt1/Robo1 gene. *Proc Natl Acad Sci U S A*. 2001;98:15062-15066.
9. Dickinson RE, Duncan WC. The SLIT-ROBO pathway: A regulator of cell function with implications for the reproductive system. *Reproduction*. 2010;139:697-704.
10. Morlot C, Thielens NM, Ravelli RB, et al. Structural insights into the Slit-Robo complex. *Proc Natl Acad Sci U S A*. 2007;104:14923-14928.
11. Xian J, Aitchison A, Bobrow L, et al. Targeted disruption of the 3 p12 gene, Dutt1/Robo1, predisposes mice to lung adenocarcinomas and lymphomas with methylation of the gene promoter. *Cancer Res*. 2004;64:6432-6437.
12. Dallol A, Krex D, Hesson L, Eng C, Maher ER, Latif F. Frequent epigenetic inactivation of the SLIT2 gene in gliomas. *Oncogene*. 2003;22:4611-4616.
13. Dallol A, Da Silva NF, Viacava P, et al. SLIT2, a human homologue of the Drosophila Slit2 gene, has tumor suppressor activity and is frequently inactivated in lung and breast cancers. *Cancer Res*. 2002;62:5874-5880.
14. Dong R, Yu J, Pu H, Zhang Z, Xu X. Frequent SLIT2 promoter methylation in the serum of patients with ovarian cancer. *J Int Med Res*. 2012;40:681-686.
15. Tseng RC, Lee SH, Hsu HS, et al. SLIT2 attenuation during lung cancer progression deregulates beta-catenin and E-cadherin and associates with poor prognosis. *Cancer Res*. 2010;70:543-551.
16. Heo DS, Snyderman C, Gollin SM, et al. Biology, cytogenetics, and sensitivity to immunological effector cells of new head and neck squamous cell carcinoma lines. *Cancer Res*. 1989;49:5167-5175.
17. White JS, Weissfeld JL, Ragin CC, et al. The influence of clinical and demographic risk factors on the establishment of head and neck squamous cell carcinoma cell lines. *Oral Oncol*. 2007;43:701-712.
18. Mitra S, Mazumder Indra D, Bhattacharya N, et al. RBSP3 is frequently altered in premalignant cervical lesions: Clinical and prognostic significance. *Genes Chromosomes Cancer*. 2010;49:155-170.
19. Sambrook JFE, Maniatis T. *Molecular Cloning: A Laboratory Manual*. Cold Spring Harbor, NY: Cold Spring Harbor Laboratory; 1989.
20. Dasgupta S, Mukherjee N, Roy S, et al. Mapping of the candidate tumor suppressor genes' loci on human chromosome 3 in head and neck squamous cell carcinoma of an Indian patient population. *Oral Oncol*. 2002;38:6-15.
21. Tripathi A, Dasgupta S, Roy A, et al. Sequential deletions in both arms of chromosome 9 are associated with the development of head and neck squamous cell carcinoma in Indian patients. *J Exp Clin Cancer Res*. 2003;22:289-297.
22. Singh RK, Indra D, Mitra S, et al. Deletions in chromosome 4 differentially associated with the development of cervical cancer: Evidence of slit2 as a candidate tumor suppressor gene. *Hum Genet*. 2007;122:71-81.
23. Maiti GP, Mondal P, Mukherjee N, et al. Overexpression of EGFR in head and neck squamous cell carcinoma is associated with inactivation of SH3 GL2 and CDC25 A genes. *PLoS One*. 2013;8:e63440.
24. Ghosh S, Ghosh A, Maiti GP, et al. Alterations of 3 p21.31 tumor suppressor genes in head and neck squamous cell carcinoma: Correlation with progression and prognosis. *Int J Cancer*. 2008;123:2594-2604.
25. Herman JG, Graff JR, Myohanen S, Nelkin BD, Baylin SB. Methylation-specific PCR: A novel PCR assay for methylation status of CpG islands. *Proc Natl Acad Sci U S A*. 1996;93:9821-9826.
26. Tripathi A, Banerjee S, Roy A, Roychowdhury S, Panda CK. Alterations of the P16 gene in uterine cervical carcinoma from Indian patients. *Int J Gynecol Cancer*. 2003;13:472-479.
27. Perrone F, Suardi S, Pastore E, et al. Molecular and cytogenetic subgroups of oropharyngeal squamous cell carcinoma. *Clin Cancer Res*. 2006;12:6643-6651.
28. Mitra S, Mazumder-Indra D, Mondal RK, et al. Inactivation of SLIT2-ROBO1/2 pathway in premalignant lesions of uterine cervix: Clinical and prognostic significances. *PLoS One*. 2012;7:e38342.
29. Narayan G, Goparaju C, Arias-Pulido H, et al. Promoter hypermethylation-mediated inactivation of multiple Slit-Robo pathway genes in cervical cancer progression. *Mol Cancer*. 2006;5:16.
30. Carmona FJ, Azuara D, Berenguer-Llergo A, et al. DNA methylation biomarkers for noninvasive diagnosis of colorectal cancer. *Cancer Prev Res (Phila)*. 2013;6:656-665.
31. Dallol A, Forgacs E, Martinez A, et al. Tumour specific promoter region methylation of the human homologue of the Drosophila Roundabout gene DUTT1 (ROBO1) in human cancers. *Oncogene*. 2002;21:3020-3028.
32. Wu WJ, Tu S, Cerione RA. Activated Cdc42 sequesters c-Cbl and prevents EGF receptor degradation. *Cell*. 2003;114:715-725.
33. Wong K, Ren XR, Huang YZ, et al. Signal transduction in neuronal migration: Roles of GTPase activating proteins and the small GTPase Cdc42 in the Slit-Robo pathway. *Cell*. 2001;107:209-221.

SUPPLEMENTARY DATA

Supplementary data related to this article can be found online at http://dx.doi.org/10.1016/j.oooo.2014.09.029

Reprint requests:

Dr. Chinmay Kumar Panda, PhD
Department of Oncogene Regulation
Chittaranjan National Cancer Institute
37, S P Mukherjee Road
Kolkata 700026
India
ckpanda.cnci@gmail.com